FATIGUE BEHAVIOUR OF A STRUCTURAL STEEL UNDER NON-PROPORTIONAL MULTIAXIAL LOADING

LUÍS REIS*, BIN LI, MANUEL de FREITAS

Department of Mechanical Engineering, Instituto Superior Técnico
Av. Rovisco Pais, 1049-001 Lisboa
E-mail: lreis@ist.utl.pt

ABSTRACT: This paper reports experimental studies on the fatigue behaviour of 42CrMo4 steel under non-proportional loading conditions. Although the 42CrMo4 steel is widely used in complex stressed components such as shafts, etc, most of the studies in the literature were on the uni-axial fatigue behaviour of this steel. The objective of this work is to study the mechanical behaviour of the steel 42CrMo4 under specified multiaxial fatigue loading conditions, which will allow a better understanding of the ratio between normal and shear stress, and validate the fatigue damage models. A series of tests were carried out in load control for several multiaxial fatigue loading paths. Experimental results show that the ratio between normal stress and shear stress components has a strong influence to fatigue damage and consequently to fatigue life. Multiaxial fatigue damage models based on the shear stress amplitude are applied to correlate the test results, improved correlation results are shown.

Keywords: Multiaxial fatigue, Non-proportional loading, Plasticity, Cyclic hardening, Multiaxial Fatigue models**.**

RESUMO: Este artigo apresenta um estudo sobre o comportamento em fadiga multiaxial do aço 42CrMo4, sob condições de carregamento não proporcional. Embora o aço 42CrMo4 seja utilizado em muitos componentes mecânicos, a maioria dos estudos referenciados na literatura apenas referem o seu comportamento em fadiga uniaxial. O objectivo deste trabalho é estudar o comportamento mecânico do aço 42CrMo4 sob condições especificas de carregamento, as quais permitirão um melhor entendimento do rácio entre a componente da tensão normal e da tensão de corte e consequentemente validar os modelos de dano à fadiga. Foram realizados vários testes, em controlo de carga, para diferentes trajectórias de carregamento. Os resultados experimentais mostram que o rácio entre a componente da tensão normal e da tensão de corte tem uma forte influência no dano à fadiga e consequentemente na vida à fadiga. São utilizados modelos de dano à fadiga multiaxial, baseados na amplitude da tensão de corte, para correlacionar com os resultados experimentais. Com o novo rácio obtém-se uma melhor correlação dos resultados.

Palavras chave: Fadiga multiaxial, Carregamento não-proporcional, Plasticidade, Encruamento cíclico, Modelos fadiga multiaxial.

1. INTRODUCTION

Engineering components in machines, vehicles and structures are generally subjected to multiaxial stress states. Under service multiaxial loading, microscopic cracks can initiate and grow until a macroscopic crack and consequently originates the damage of the component and/or structure. The behaviour of crack initiation and propagation until final fracture of materials under multiaxial stress states is quite different from that under uniaxial stress state, therefore, multiaxial fatigue has become a very active topic in the past 20 years, because of the great importance in mechanical design.

There are many multiaxial fatigue models proposed in the literature, and many corresponding approaches have been developed for evaluating the shear stress amplitude under multiaxial fatigue loading conditions. For efficient computational fatigue analysis of components and structures, it is required to carry out further validations of multiaxial fatigue models and appropriate approaches for shear stress evaluation under service loading conditions [1].

For structural steels, the shear stress amplitude is one of the most important parameters in the formulations of multiaxial fatigue damage models. Conventionally, the shear stress amplitude was usually evaluated in the shear stress space based on the von Mises equivalence ($\tau=\sigma/\sqrt{3}$) or the Tresca equivalence ($\tau=\sigma/2$) for the multiaxial loading conditions. However, the relationship of the equivalent shear stress related to the axial stress component may vary significantly depending on the type of the material. For example, the ratio of the torsion fatigue limit over the bending fatigue limit τ_{-1}/f_{-1} varies from 0.5 for mild metals to 1 for brittle metals [2].

In this paper, systematic fatigue experiments are presented for a structural steel, 42CrMo4, quenched and tempered steel, under typical axial-torsional multiaxial loading paths

(a lozenge, a rectangle and an ellipse). Tests were carried out in high cycle fatigue regime, 10^5 – 10^7 cycles.

It is proposed to evaluate the shear stress amplitude in the stress space appropriate to the material type. For the 42CrMo4 steel studied, the shear stress space with the equivalence (τ=0.65*σ) is used for the shear stress amplitude evaluations under multiaxial loading conditions. The MCE (Minimum Circumscribed Ellipse) approach, developed by the authors [3], previously, is used for evaluating the shear stress amplitude and correlating experimental results. Improved correlations are shown.

2. MATERIAL DATA, SPECIMEN FORM AND TEST PROCEDURE

The material studied in this paper is the 42CrMo4 quenched and tempered high strength steel. The chemical composition is shown in Table 1. In order to characterize the cyclic stress-strain behaviour of the material studied, tension-compression low cycle fatigue tests were carried out. Monotonic and cyclic mechanical properties are shown in Table 2 (cyclic properties obtained by fitting the test results). The geometry and dimensions of the specimen are shown in Fig. 1.

Table 1 – Chemical composition of the material studied 42CrMo4 (in wt%).

C	Si	Mn	P	S	Cr	Ni	Mo	Cu
0.39	0.17	0.77	0.025	0.02	1.1	0.3	0.16	0.21

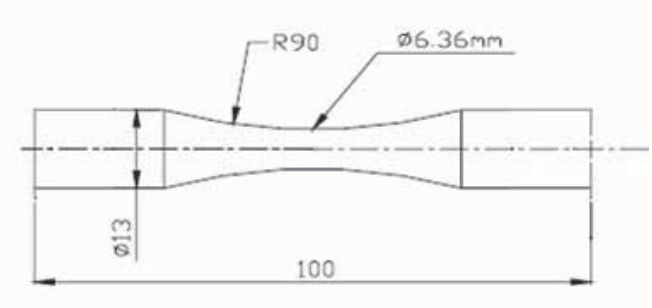

Fig. 1. Specimen geometry for biaxial cyclic tension-compression with cyclic torsion tests.

Table 2 – Monotonic and cyclic mechanical properties of the material studied.

Tensile Strength, σ (MPa)	1100
Yield Strength, $\sigma_{0.2}$ (MPa)	980
Elongation, A (%)	16
Cyclic Yield Strength, $\sigma_{p0.2,cyclic}$ (MPa)	540
Strength coefficient, K´ [MPa]	1420
Strain hardening exponent, n´	0.12
Fatigue strength coefficient, σ_f´ (MPa)	1154
Fatigue strength exponent, b	-0.061
Fatigue ductility coefficient, ε_f´	0.18
Fatigue ductility exponent, c	-0,53

Tests of biaxial cyclic tension-compression with cyclic torsion were performed on a biaxial servo-hydraulic machine, shown in Fig. 2. Test conditions were as follows: frequency 4-6 Hz at room temperature and laboratory air. Tests ended up when the specimens were completely broken.

To study the effects of the multiaxial loading paths and in particular both the effect of axial component and the effect of torsional component on the fatigue life, a series of loading paths were applied in the experiments as shown in Tables 3 and 4.

Table 3 – Reference multiaxial fatigue loading paths.

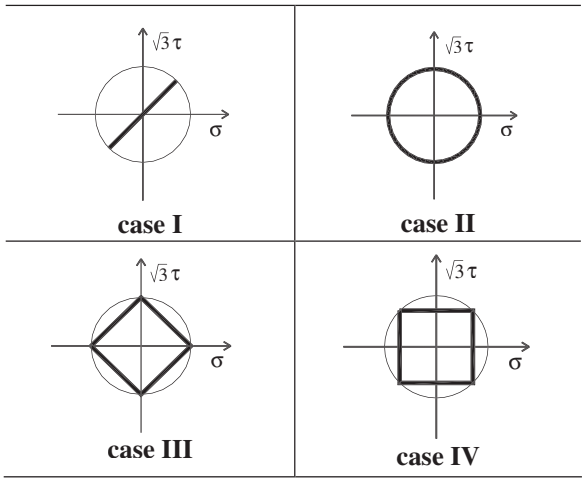

Table 4 – Variations of the reference multiaxial fatigue loading paths.

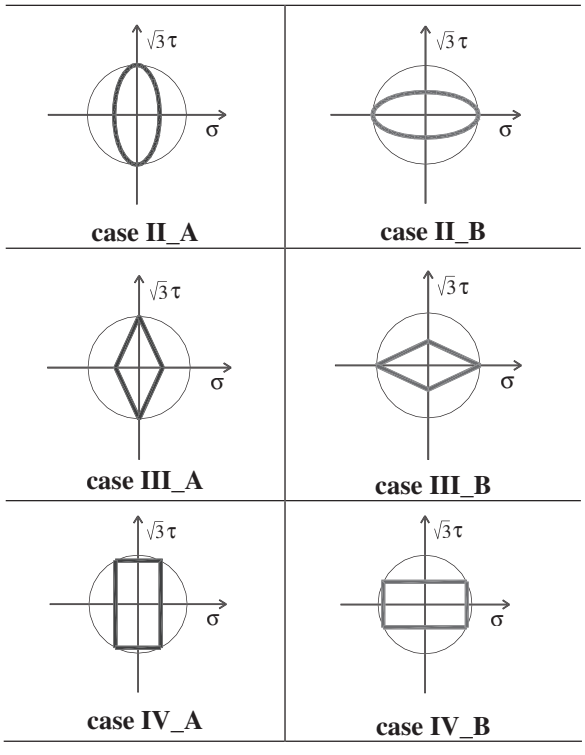

Fig. 2. Biaxial testing machine (Instron 8874).

3. THEORETICAL ANALYSIS: EVALUATION OF THE SHEAR STRESS AMPLITUDE

Many multiaxial fatigue models have been proposed in the last decades [1]. Among several parameters and constants the shear stress amplitude is one of the most important parameters in the formulations of the multiaxial fatigue damage models, in high cycle fatigue regime.

Among many multiaxial models, the Sines [4] and the Crossland [5] are two important criteria, which are formulated by the amplitude of the second deviatoric stress invariant and the hydrostatic stress P_H:

$$\sqrt{J_{2,a}} + k(N)P_H = \lambda(N) \qquad (1)$$

where $k(N)$ and $\lambda(N)$ denote material parameters for a given life N.

Crossland suggested using the maximum value of the hydrostatic stress $P_{H,max}$ instead of the mean value of hydrostatic stress $P_{H,m}$ used by Sines in the Eq.(1). A physical interpretation of the criterion expressed in Eq.(2) is the follow: for a given cyclic life N, the permissible amplitude of the root-mean-square of the shear stress over all planes is a linear function of the normal stress averaged over all planes. Besides, from the viewpoint of computational efficiency, the stress-invariant based approach such as Eq. (1) it is easy to use and computationally efficient.

In practical engineering design, the Sines and Crossland criteria have found successful applications for proportional multiaxial loading. For non-proportional multiaxial loading, it has been shown that the Sines and Crossland criteria can also yield better prediction results by using improved method MCE for evaluating the effective shear stress amplitude of the non-proportional loading path.

The evaluation of shear stress amplitude is a key issue for fatigue estimations using Eq. (1). The definition of the square root of the second invariant of the stress deviator is:

$$\sqrt{J_2} \equiv \sqrt{\frac{1}{6}\left\{\left(\sigma_{xx}-\sigma_{yy}\right)^2+\left(\sigma_{yy}-\sigma_{zz}\right)^2+\left(\sigma_{zz}-\sigma_{xx}\right)^2\right\}+\sqrt{\left\{\left(\sigma_{xy}\right)^2+\left(\sigma_{yz}\right)^2+\left(\sigma_{zx}\right)^2\right\}} \qquad (2)$$

One direct way to calculate the amplitude of $\sqrt{J_2}$ is:

$$\sqrt{J_{2,a}} \equiv \sqrt{\frac{1}{6}\left\{\left(\sigma_{xx,a}-\sigma_{yy,a}\right)^2+\left(\sigma_{yy,a}-\sigma_{zz,a}\right)^2+\left(\sigma_{zz,a}-\sigma_{xx,a}\right)^2\right\}+\sqrt{\left\{\left(\sigma_{xy,a}\right)^2+\left(\sigma_{yz,a}\right)^2+\left(\sigma_{zx,a}\right)^2\right\}} \qquad (3)$$

Eq.(3) is applicable for proportional loading, where all the stress components vary proportionally. However, when the stress components vary non-proportionally (for example, with phase shift between the stress components), Eq.(3) gives the same result with that of proportional loading condition. In fact, the non-proportionality has influence on the shear stress amplitude generated by multiaxial loading. Therefore, a new methodology is needed.

3.1 Equivalent Stress Range of ASME Code

The ASME Boiler and Pressure Vessel code Procedure [6] is based on the von Mises hypothesis, but employs the stress difference $\Delta\sigma_i$ between to two arbitrary instants t_1 and t_2:

$$\Delta\sigma_{eq} = \frac{1}{2\sqrt{2}}\left\{\left(\Delta\sigma_x-\Delta\sigma_y\right)^2+\left(\Delta\sigma_y-\Delta\sigma_z\right)^2+\left(\Delta\sigma_z-\Delta\sigma_x\right)^2+6\left(\Delta\tau_{xy}{}^2+\Delta\tau_{yz}{}^2+\Delta\tau_{xz}{}^2\right)\right\}^{1/2} \qquad (4)$$

where the equivalent stress range $\Delta\sigma_{eq}$ is maximized with respect to time. Eq. (4) produces a lower equivalent stress range, for some conditions, in out-of-phase than the in-phase loading, leading an increase of the fatigue life, which is in contradiction with experimental results.

3.2. MCE Approach for evaluating shear stress amplitude

The longest chord (LC) approach is one of the well-known approaches as summarized by Papadopoulos [2], which defines the shear stress amplitude as half of the longest chord of the loading path, denoted as D/2.

The MCC approach [2] defines the shear stress amplitude as the radius of the minimum circle circumscribing to the loading path. On the basis of MCC approach, a new approach, called the minimum circumscribed ellipse (MCE) approach [3], was proposed to compute the effective shear stress amplitude taking into account the non-proportional loading effect.

The load traces are represented and analyzed in the transformed deviatoric stress space, where each point represents a value of $\sqrt{J_2}$ and the variations of $\sqrt{J_2}$ are

shown during a loading cycle. The schematic representation of the MCE approach and the relation with the minimum circumscribed circle (MCC) approach are illustrated in Fig. 3:

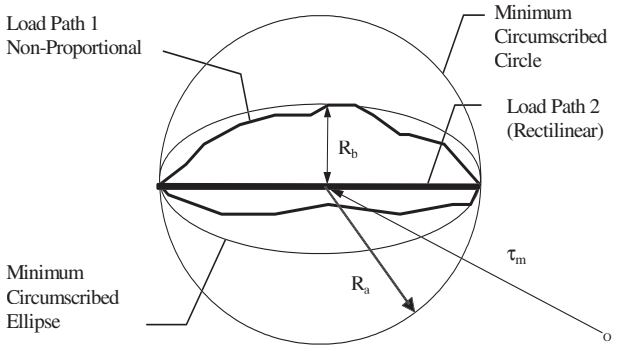

Fig. 3. The MCC and MCE circumscribing to shear stress traces, R_a and R_b are the major and minor radius of MCE, respectively.

The idea of the MCE approach is to construct a minimum circumscribed ellipse that can enclose the whole loading path throughout a loading block in the transformed deviatoric stress space.

Rather than defining $\sqrt{J_{2,a}} = R_a$ by the minimum circumscribed circle (MCC) approach, a new definition of $\sqrt{J_{2,a}}$ was proposed [3], where R_a and R_b are the lengths of the major semi-axis and the minor semi-axis of the minimum circumscribed ellipse respectively.

The ratio of R_b/R_a represents the non-proportionality of the shear stress path. The important advantage of this new MCE approach is that it can take into account the non-proportional loading effects in an easy way.

As shown in Fig. 3, for the non-proportional loading path 1, the shear stress amplitude is defined as:

$$\sqrt{J_{2,a}} = \sqrt{R_a^2 + R_b^2} \qquad (5)$$

For the proportional loading path 2, it is defined as $\sqrt{J_{2,a}} = R_a$ since R_b is equal to zero (rectilinear loading trace).

4. RESULTS AND DISCUSSIONS

4.1. Experimental cyclic stress-strain behavior under proportional and non-proportional loading with von Mises parameter

Proportional and non-proportional cyclic tests were conducted in the plane (σ, $\sqrt{3}\tau$). Non-proportional cyclic tests were conducted with the square, rectangle up and rectangle down, circle, ellipse down, ellipse up, lozenge, lozenge up and lozenge down loading paths, respectively (see Tables 3 and 4). Fig.(s) 4 and 5 show the evolution of experimental life with equivalent von Mises stress parameter for cases I, II, II_A, II_B, III, III_A and III_B.

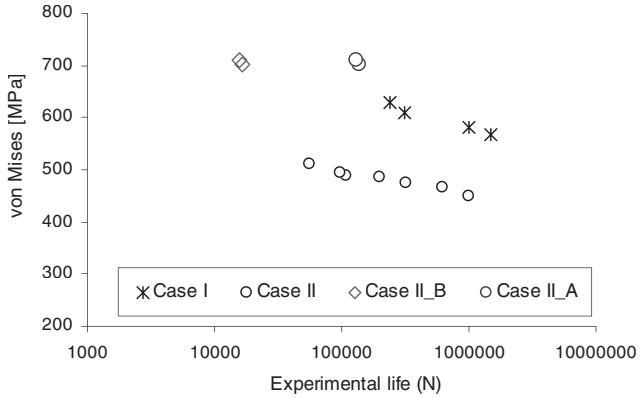

Fig. 4. Evolution of experimental life with equivalent von Mises stress: cases I, II, II_A and II_B, respectively.

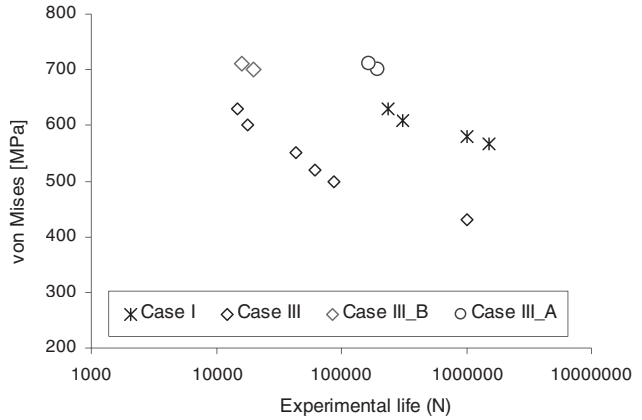

Fig. 5. Evolution of experimental life with equivalent von Mises stress: cases I, III, III_A and III_B, respectively.

From Fig.(s) 4 and 5 it is shown that the von Mises parameter gives a big scatter when correlating the experimental results. In both pictures, it seems that there's two tendencies, one for proportional loading, case I, with cases II_A and III_A (strong torsional component) and another one with cases II, III, II_B and III_B (strong axial component). Can also be observed that cases II_A and III_A are least severe together with the proportional case I. This means that a bigger torsional component, as compared with the axial one, has not so strong influence in the fatigue life strength.

5.2. Experimental cyclic stress-strain behavior under proportional and non-proportional loading with new fatigue parameter

Fig.(s) 6 and 7 show the evolution of experimental life with the new parameter for cases I, II, II_A, II_B, III, III_A and III_B.

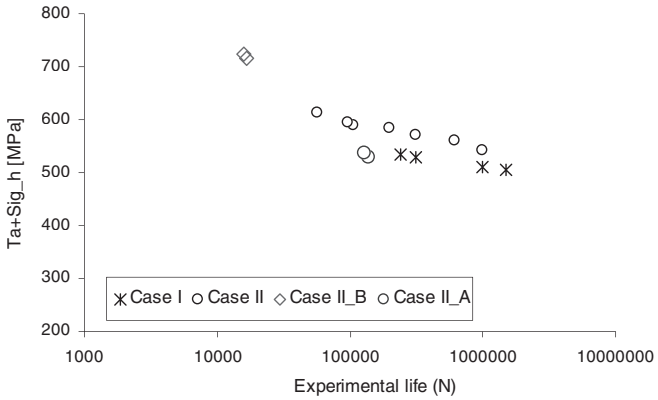

Fig. 6. Evolution of the new fatigue parameter with experimental life: cases I, II, II_A and II_B, respectively.

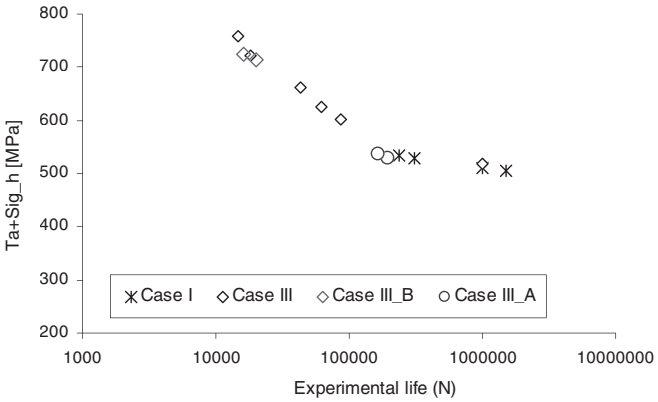

Fig. 7. Evolution of the new fatigue parameter with experimental life: cases I, III, III_A and III_B, respectively.

In order to get better correlations, the new shear stress space parameter with the equivalence $\tau=0.65*\sigma$ is used for the shear stress amplitude evaluations under multiaxial loading conditions. The parameter (Ta+Sig_h) is obtained from Eq. (2) with the shear stress amplitude calculated from Eq. (5). Fig. (s) 6 and 7, show the improved correlations obtained with the new parameter, presented in this paper. There's a good correlation between the different cases, which can be observed from the position of the data and corresponding to a unique tendencies.

Fig. 8 present all the results obtained from the variations of the reference multiaxial fatigue loading paths (Table 4). It can be observed that there's a good correlation between the data. The present work is part of continuous research in this matter and these results give some confidence in the upcoming work.

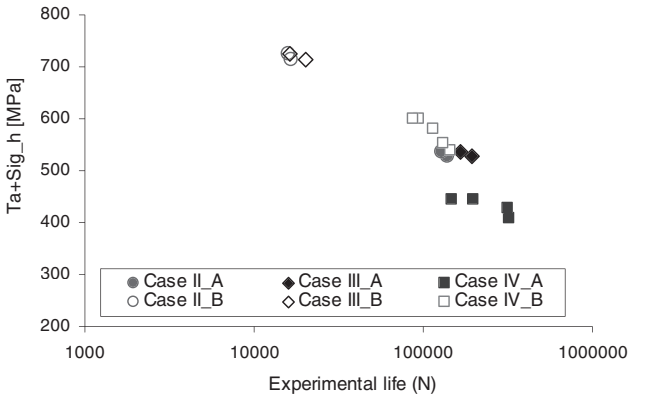

Fig. 8. Evolution of the new fatigue parameter with experimental life: cases II_A, II_B, III_A, III_B, IV_A and IV_B, respectively.

5. CONCLUSIONS

Experimental results show that the ratio between normal stress component and shear stress component has a strong influence to fatigue damage and consequently in fatigue life.

The shear stress space used for the evaluation of the shear stress amplitude of multiaxial loading conditions should be appropriate for this material type.

ACKNOWLEDGEMENTS

Financial support of this work by FCT - Fundação para Ciência e Tecnología (Portuguese Foundation for Science and Technology) is gratefully acknowledged through the project PPCDT/EME/59577/2004.

REFERENCES

[1] Socie D. F. and Marquis G. B. Multiaxial Fatigue, SAE, Warrendale, PA 15096-0001, (2000).

[2] Papadopoulos, I.V., Davoli, P., Gorla, C., Fillipini, M.and Bernasconi, A. A comparative study of multiaxial high-cycle fatigue criteria for metals. International Journal of Fatigue, Vol. 19, Nº3, pp. 219-235, (1997).

[3] M. de Freitas, B. Li and J.L.T. Santos, Multiaxial Fatigue and Deformation: Testing and Prediction, ASTM STP 1387, S. Kaluri and P.J. Bonacuse, Eds., ASTM, West Consh, PA, pp.139-156. (2000).

[4] Sines, G., Metal Fatigue, (edited by G. Sines and J.L.Waisman), McGraw Hill, N.Y, pp.145-169, (1959).

[5] Crossland, B., Proc. Int. Conf. on Fatigue of Metals, Inst. of Mech. Eng, London, pp.138-149, (1956).

[6] ASME Code Case N-47-23 (1988) Case of ASME Boiler and Pressure Vessel Code, ASME.